Cyclooxygenase and CD147 expression in oral squamous cell carcinoma patient samples and cell lines

Walaa Hamed Shaker Nasry, MB, BCh, MSc,[a] Haili Wang, MSc,[a] Kathleen Jones, BSc, MLT,[b] Marvin Tesch, MD,[c] Juan Carlos Rodriguez-Lecompte, DVM, PhD,[a] and Chelsea K. Martin, DVM, PhD[a]

Objectives. In oral squamous cell carcinoma (OSCC), cyclooxygenases (COX-1 and COX-2) contribute to inflammation, and cluster of differentiation factor 147 (CD147) contributes to invasiveness, but their relationship has not been previously examined within a cohort of patients with OSCC or OSCC cell lines.

Study Design. COX-2 and CD147 expression was determined by using immunohistochemistry on 39 surgical biopsy specimens of OSCC. Expression in tumor cells, stroma, and adjacent oral epithelium was characterized by using a visual grading system. COX-1, COX-2, and CD147 expression was determined in vitro by using OSCC cell lines (SCC25, BHY, and HN) and reverse transcriptase-quantitative polymerase chain reaction. Secretion of prostagladin E_2 (PGE_2) from OSCC cell lines was determined by using PGE_2 enzyme-linked immunosorbent assay.

Results. Biopsy specimens showed higher COX-2 expression in tumor cells compared with stroma and adjacent epithelium ($P < .05$). There was no difference in CD147 expression among the tumor cells, stroma, and adjacent epithelium. In OSCC cell lines, there was a trend for COX-2 and CD147 gene expression to be coordinated. Interestingly, PGE_2 secretion was more closely related to COX-1 expression than to COX-2 expression.

Conclusions. COX-1, COX-2, and CD147 appear to be independently regulated in OSCC, potentially representing 2 therapeutic targets for future investigation. COX-1 expression in OSCC deserves further study because it may be an important determinant of PGE_2 secretion from OSCC cells. (Oral Surg Oral Med Oral Pathol Oral Radiol 2019;128:400−410)

Squamous cell carcinomas (SCC) account for 90% of malignancies in the upper aerodigestive tract.[1] It is a very aggressive form of cancer, often diagnosed late in the disease course,[2] with an overall 5-year survival rate of only 63%.[3] Oral and oropharyngeal squamous cell carcinoma is the sixth most common cancer, after lung, stomach, breast, colorectal, and cervical cancers.[1,4] According to the Canadian Cancer Society, it was estimated that 4700 Canadians (3200 men and 1450 women) were diagnosed with oral cavity cancer in 2017, with 1250 Canadians dying of the disease.[5] Globally, 300,400 new cases and 145,400 deaths from oral cavity cancer (including lip cancer) occurred in 2012.[6] Oral cancer is more common in developing countries compared with developed countries, with the highest rates of occurrence reported in Pakistan, India, Brazil, Thailand, and Slovakia.[7] In the United States, approximately 41,380 new cases and 7890 deaths are reported every year.[8]

Oral cancer invades the underlying tissue, including maxillary and mandibular bone,[9] as well as metastasizing to regional lymph nodes and lungs.[10] Factors that enable oral squamous cell carcinoma (OSCC) invasion and intravasation into the lymphatics and blood vessels include inflammatory mediators, such as prostaglandin E_2 (PGE_2),[11,12] as well as matrix metalloproteinase (MMP) enzymes under the regulation of cluster of differentiation factor 147 (CD147).[13]

PGE_2 is a mediator of active inflammation, promoting local vasodilation and local attraction and activation of neutrophils, macrophages, and mast cells in the early stages of acute inflammation.[14] Although inflammatory cells are an important source of PGE_2, this inflammatory eicosanoid can be released by a variety of cell types.[14] PGE_2 synthesis starts with liberation of arachidonic acid (AA) from the cell membrane.[15,16] AA is then converted into prostaglandin H_2 by cyclooxygenase 1 and 2 (COX-1 and COX-2) enzymes, which is then rapidly converted into PGE_2 by microsomal and cytosolic PGE_2 synthase enzymes.[15,16] We have recently reviewed the role of the AA pathway of inflammation in the pathogenesis of

Statement of Clinical Relevance

The arachidonic acid pathway and cluster of differentiation factor 147 may represent 2 separate therapeutic targets for oral squamous cell carcinoma (OSCC). Furthermore, cyclooxygenase-1 (COX-1) appears to be an important source of OSCC-derived prostaglandin E_2, and therefore should not be overlooked in future studies of COX inhibitor-based therapies.

[a]Department of Pathology and Microbiology, Atlantic Veterinary College, University of Prince Edward Island, Charlottetown, Prince Edward Island, Canada.
[b]Diagnostic Services, Atlantic Veterinary College, University of Prince Edward Island, Charlottetown, Prince Edward Island, Canada.
[c]Provincial Health Services, Health PEI, Charlottetown, Prince Edward Island, Canada.
Received for publication Jan 2, 2019; returned for revision May 9, 2019; accepted for publication Jun 5, 2019.

2212-4403/$-see front matter
https://doi.org/10.1016/j.oooo.2019.06.005

OSCC,[17] which is related to chronic tobacco and alcohol use in patients with oral cancer.[18]

Protumorigenic functions of the AA cascade serve as a therapeutic target, with nonsteroidal anti-inflammatory drugs demonstrating the ability to suppress carcinogenesis and tumor cell proliferation.[19-21] The combination of celecoxib (a COX-2 inhibitor), erlotinib (an epidermal growth factor receptor tyrosine kinase inhibitor), and radiation therapy has shown activity against recurrent OSCC.[22]

Invasion of tumor cells, including OSCC, requires extensive proteolysis of the extracellular matrix. This process is accomplished with MMPs, with MMP2 and MMP9 proving to be particularly important.[23] MMP expression in patients with cancers, including pancreatic, colorectal, breast, and cervical cancers and OSCC, have been linked to decreased survival.[24,25] CD147, also referred to as *Basigin* and *extracellular matrix metalloproteinase inducer (EMMPRIN)*, activates MMPs and contributes to tumor invasion.[26]

CD147 plays an important role in immunity and inflammation, with increased expression in a variety of inflammatory cells.[27,28] A direct relationship between the AA pathway and CD147 was demonstrated in atherosclerotic plaques, where COX-2 stimulated CD147 expression through production of PGE_2.[29]

An association between increased CD147 expression and poor prognosis has been demonstrated in a variety of cancers, such as OSCC.[30] CD147 activation of MMPs in the tumor microenvironment causes tumor cells to invade the surrounding stroma.[31] For example, CD147 inhibition resulted in decreased expression of inflammatory mediators in a mouse model of OSCC and also reduced collagen degradation and tumor cell growth in vitro.[32] In hypopharyngeal SCC, COX-2 and CD147 were associated with tumor invasion, lymph node metastasis, and poor patient survival.[33] Furthermore, anti-CD147 therapy was shown to reduce tumor growth in a xenograft mouse model of OSCC.[32]

The purpose of this study was to explore the relationship between COX-2 and CD147 expression in OSCC by using archival biopsy samples from patients with OSCC in Eastern Canada, as well as in 3 human OSCC cell lines representing lingual OSCC (SCC25), highly invasive gingival OSCC (BHY), and an OSCC metastasis isolated from a regional lymph node (HN).

MATERIALS AND METHODS

Immunohistochemical detection of COX enzymes and CD147 in human OSCC biopsies

Patient signalment and biopsy information. Archival, formalin-fixed paraffin-embedded biopsy samples representing 39 cases of human OSCC were obtained from Health PEI Laboratory Services (Charlottetown, Prince Edward Island, Canada). Biopsy samples were collected between 2008 and 2015, and the diagnosis of OSCC was confirmed by a medical pathologist before inclusion in the study. Most patients were male (28 of 39), and most patients were 50 to 79 years of age (30 of 39). The biopsy specimens were obtained from a variety of locations in the oral cavity, with OSCC of the tongue being the most common (27 of 39) (Table I). Use of biopsy specimens for this study was approved by the Prince Edward Island Research Ethics Board and the University of Prince Edward Island Research Ethics Board. Of the 39 OSCC slides, 2 were not evaluated for COX-2 expression because of loss of tissue during the staining process.

Primary antibodies and matching isotype control antibodies. Immunohistochemistry protocols were designed for the detection of COX-2 and CD147 by using a polyclonal rabbit anti-COX-2 (mouse) immunoglobulin G (IgG) (Cayman Chemical Company, Ann Arbor, MI) and polyclonal goat anti-CD147 (human) IgG (Santa Cruz Biotechnology Inc., Dallas, TX). The concentration of normal rabbit IgG (Millipore Sigma Company, Etobicoke, Ontario, Canada) and normal goat IgG (Santa Cruz Biotechnology Inc.) were matched to the concentration of the primary antibody (100 μg/mL for COX-2 and 200 μg/mL for CD147). Human seminal vesicle was selected as a positive control tissue for COX-2 expression,[34] and human small intestine was selected as positive control tissue for CD147 expression.[35] (Supplemental Figure 1). An immunohistochemistry protocol for detection of COX-1 was also investigated by using a polyclonal rabbit anti-COX-1 (ovine) antiserum (Cayman Chemical Company) and normal rabbit serum (negative control) at a dilution 1:100, using feline intestinal goblet cells as a positive control,[36] but staining was similar between the positive and negative controls (see Supplemental Figure 1), so COX-1 immunohistochemistry was not pursued.

Immunohistochemistry protocol. Standard horseradish peroxidase immunohistochemistry was performed to detect COX-2 and CD147 expression in OSCC biopsy specimens. Briefly, 5-μm thick tissue sections were deparaffinized with xylene (Fisher Scientific, Waltham, MA) and rehydrated through diminishing concentrations of ethanol in water. Antigen retrieval was

Table I. Oral squamous cell carcinoma (OSCC) cases

Gender	*(n)*	*Age (years)*	*(n)*	*Tumour location*	*(n)*
Male	28	40–49	3	Gingiva	2
Female	11	50–59	10	Oral mucosa	5
		60–69	10	Tongue	27
		70–79	10	Buccal Mucosa	2
		≥80	6	Larynx	1
				Tonsils	1
				Epiglottis	1

achieved by incubating the slides in (95˚C) sodium citrate buffer (pH 6.0) for 20 minutes in a steamer (Black and Decker, Mississauga, Ontario), followed by 20 minutes of cooling at room temperature. Endogenous peroxidases were quenched for 20 minutes with an incubation in 3% hydrogen peroxide (Fisher Scientific). Endogenous avidin and biotin was blocked by using a commercially available kit, according to manufacturer instructions (Vector Laboratories, Burlington, Ontario, Canada). Slides were incubated with primary antibodies or negative control antibodies (normal IgG) for 60 minutes at room temperature in a humidified chamber, followed by 30 minutes incubation with biotinylated goat anti-rabbit IgG (for COX-2) or rabbit anti-goat IgG (for CD147) (Vector Laboratories). Visualization of signal was achieved with Vectastain ABC reagent (Vector Laboratories) followed by diaminobenzinetetrahydrochloride (DAB) solution (Vector Laboratories). The duration of DAB incubation was determined through pilot experiments and was then held constant for all slides. Between each step, slides were washed with phosphate-buffered saline (Fisher Scientific). The sections were counterstained with hematoxylin, dehydrated with ethanol and xylene, and cover-slipped by using a xylene-based mounting medium (Fisher Scientific).

The specificity of secondary antibodies was evaluated by omitting the primary antibody from the protocol on a subset of slides. Additionally, the specificity of the protocol was evaluated by incubating positive control tissues and a subset of OSCC samples with matching normal IgG or antiserum (Supplemental Figure 2), or preadsorbing the primary antibody with the appropriate peptide (COX-2). Optimization of the protocols included testing several concentrations of primary antibody and duration of DAB incubation. The range of dilutions tested for the primary antibodies were 1:200 and 1:100 for COX-2; 1:1000, 1:500, 1:400, 1:200, 1:100, and 1:40 for COX-1; and 1:200, 1:100 and 1:50 for CD147. The duration of DAB incubation ranged from 2 minutes to 10 minutes in optimization experiments before arriving at 1 minute and 20 seconds for COX-1, 1 minute and 30 seconds for COX-2, and 3 minutes and 40 seconds for CD147. Protocols that yielded signals on positive control tissue and those with minimal nonspecific staining were selected for evaluating human OSCC specimens. Positive and negative controls were run with all OSCC slides.

Immunohistochemistry grading system. A visual grading system that distinguished between tumor and stroma (and adjacent epithelium, if present) was used. The percentage of positive cells in the tumor cells, adjacent epithelium, and supporting tumor stroma, along with staining intensity, were estimated and converted into a categorical grading system (Table II).

Table II. Immunohistochemistry grading system

Grade	*Description*
Negative	Less than 1% positive cells
Grade 1	1%−9% positive cells (light, moderate or heavy staining)
Grade 2	10%−50% light cells with scattered moderate or heavy staining
Grade 3	Mostly light staining, with less than 50% moderate staining, and scattered heavy staining
Grade 4	Mostly moderate staining, with less than 50% heavy staining

Gene expression of COX enzymes and CD147 in OSCC cell lines

Cell lines, reagents, and primers. Commercially available human OSCC cell lines used in this study included: SCC25 from the tongue of a 70-year-old man (American Type Culture Collection, Manassas, VA); HN from lymph node metastasis of a 60-year-old man; and BHY from gingiva of a 52-year-old man (Leibniz Institute DSMZ-German Collection of Microorganisms and Cell Cultures, Braunschweig, Germany). The BHY and HN cells were maintained in growth medium consisting of 90% Dulbecco's modified Eagle medium (4.5 g/L glucose, HyClone Laboratories, South Logan, UT) and 10% heat inactivated fetal bovine serum (FBS, HyClone Laboratories), 100 units/mL penicillin and 100 μg/mL streptomycin (HyClone Laboratories). SCC25 cells were maintained in growth medium consisting of a 1:1 mixture of Dulbecco modified Eagle medium and Ham's F12 medium containing 2.5 mM L glutamine, 15 mM hydroxyethyl-piperazineethane−sulfonic acid buffer, and 0.5 mM sodium pyruvate (Fisher Scientific) and supplemented with 400 ng/mL hydrocortisone (HyClone Laboratories), 10% FBS, 100 units/mL penicillin and 100 μg/mL streptomycin. The cell lines were periodically split by using 0.25% trypsin-ethylenediaminetetraacetic acid (Wisent Inc., Saint-Jean-Baptiste, Quebec, Canada).

Commercially available prevalidated primers for human genes were purchased from Bio-Rad Laboratories (Mississauga, Ontario, Canada). Supplemental Table I shows 14 candidate reference (housekeeping) genes were screened by testing 6 cDNA samples representing the 3 human cell lines and 2 experimental conditions (serum deprivation and serum stimulation) on a predesigned 96-well panel (Reference Genes H96, Bio-Rad Laboratories). On the basis of acceptable gene stability values (M) and coefficients of variation determined by using CFX Manager 3.1 (Bio-Rad Laboratories), 5 candidate human reference genes were selected for additional evaluation in the full gene expression study. Primer information for the 3 genes of interest (*COX-1, COX-2*, and *CD147*) and the candidate reference genes (*TBP, RPS18, HPRT1, GAPDH*, and *B2M*) are listed in Supplemental Table II.

M and coefficients of variation values for the reference genes were revaluated in the final data sets, with the best reference genes selected for normalization of the data (*RPS18* and *HPRT1*).

Experimental conditions, RNA extraction, and cDNA synthesis

To determine the expression of COX enzymes and CD147 in OSCC cell lines, reverse transcriptase-quantitative polymerase chain reaction (RT-qPCR) was performed. OSCC cells (2×10^5) were seeded into each well of a 6-well plate (Fisher Scientific), grown for 48 hours and rinsed with sterile phosphate-buffered saline before overnight culture in serum free medium containing 0.1% bovine serum albumin (HyClone Laboratories). The next morning, the serum deprivation group remained in the serum free medium for an additional 2 hours, whereas the medium for the serum stimulated group was replaced with standard growth medium containing 10% FBS and cultured for 2 hours. This protocol provided cultures that were approximately 80% confluent at the time of RNA extraction. All cultures were performed in triplicate, and 3 independent experiments were performed.

RNA was extracted by using the Aurum total RNA mini kit (Bio-Rad Laboratories), according to the manufacturer's instructions. RNA concentration and A260/A280 ratios were determined by using the NanoDrop ND-1000 spectrophotometer (Thermo Scientific, Rockford, IL). Isolated RNA was stored at −80˚C until used for RT-qPCR. RNA samples were reverse-transcribed by using the iScript gDNA Clear cDNA Synthesis Kit (Bio-Rad Laboratories), according to the manufacturer's instructions (250 ng of RNA in a 20 μL reaction volume). To test for genomic DNA contamination, no-reverse-transcriptase (NRT) controls were prepared on a subset of samples. The thermal MyCycler (Bio-Rad Laboratories) was used for the synthesis reaction (5 minutes at 25˚C, reverse transcription for 20 minutes at 46˚C, and RT inactivation for 1 minute at 95˚C). cDNA was stored at −20˚C until used for real-time RT-qPCR.

RT-qPCR optimization. RT-qPCR was performed according to the manufacturer's instructions (Bio-Rad Laboratories), and consisted of a 10 μL reaction volume, containing 0.5 μL of proprietary primer mixture (Bio-Rad Laboratories), 5 μL of Sso Advanced Universal SYBR Green Supermix (Bio-Rad Laboratories), and 4.5 μL of diluted cDNA (or NRT or water). Real-time RT-qPCR was performed by using a CFX96 Real−Time PCR Machine (Bio-Rad Laboratories). Validation of primers included evaluation of thermal gradients to identify ideal annealing temperature (52˚C−64˚C), melt curve analysis, evaluation of amplicon size with use of agarose gel electrophoresis, and standard curves to determine reaction efficiency. Optimization steps utilized pooled cDNA samples representing all the samples in the experiment. Additionally, appropriate performance in NRT and no-template control samples was confirmed. For no-template control reactions, cDNA was replaced with nuclease free water.

To determine the reaction efficiencies of the primers, serial dilutions of pooled cDNA were prepared from the cell line samples. Dilution series ranged from 2-fold dilution series to 4-fold dilution series, depending on the Cq values generated during the thermal gradient experiment. The efficiency of the optimized RT-qPCR assays was determined by using CFX Manager 3.1 (Bio-Rad Laboratories). Target amplification efficiency for the reactions ranged from 90% to 110%. Finalized RT-qPCR protocols used cDNA diluted 1:16 (COX-1, COX-2, CD147, TBP, and HPRT1) and 1:64 (B2M, GAPDH, and RPS18). All of the samples in each experiment were run in technical duplicates (2 reaction wells per sample generating an average Cq value). Reaction protocols started with a 3-minute 95˚C denaturation step, followed by 40 cycles consisting of 5 seconds of denaturation at 95˚C, 20 seconds of annealing at 60˚C, and 20 seconds of extension at 72˚C. The reaction protocol was completed with a melt curve analysis, where the temperature was raised from 65˚C to 95˚C in 0.5˚C, 5-second increments.

Enzyme-linked immunosorbent assay (ELISA) detection of PGE_2 in OSCC cell lines

To measure PGE_2 secretion, OSCC cells were seeded into a 6-well plate at a density of 5×10^5 cells per well. OSCC cells were cultured in growth medium, as described above, for 48 hours, followed by collection of conditioned medium and determination of cell numbers by manual counting after trypsinization. Three independent experiments were performed, with each experiment including triplicate culture wells. PGE_2 concentration was measured by using a Prostaglandin E_2 Multispecies Competitive ELISA Kit (Thermo Scientific) according to the manufacturer's instructions. PGE_2 concentration was calculated from a standard curve and normalized to the average number of cells in the cultures at the time of supernatant collection.

Statistical analysis

All statistical analyses were carried out by using Stata IC 14 software (StataCorp LLP, College Station, TX). *P* values of 0.05 or less were considered statistically significant. Fisher's exact test was used for immunohistochemistry data. RT-qPCR data were tested for normality by using the Shapiro-Wilk test, followed by the Kruskal-Wallis test and graphically represented by showing relative expression compared with a low-expressing cell line. ELISA data

were log-transformed and then tested for normality by using the Shapiro-Wilk test, followed by 1-way analysis of variance and Bonferroni post hoc test. In vitro data from 3 independent experiments were combined for statistical analysis. Bar graphs show means with standard deviation.

RESULTS

COX-2 and CD147 expression in OSCC biopsy specimens

Serial sections of OSCC were evaluated for COX-2 and CD147 expression by using immunohistochemistry, which revealed variable expression levels of both targets. COX-2 was chiefly localized to the cytoplasm of tumor cells and occasionally observed within the nucleus. CD147 expression was more widespread, with expression in tumor cells and within the cells of the microenvironment (stromal fibroblasts, immune cells, and endothelial cells). CD147 localization was cytoplasmic, membranous, and nuclear in some cells (Figure 1). Thirty-seven OSCC biopsy specimens were stained for COX-2. COX-2 expression was generally of low intensity but was expressed in tumor cells more often compared with surrounding stroma or adjacent epithelium. Of the biopsy specimens, 29.7% had grade 1 and 5.4% had grade 2 staining in the tumor cells, compared with only 3.6% of specimens having grade 1 staining in adjacent epithelium and none having detectable COX-2 expression in the surrounding stroma ($P < .05$; Figure 2A). CD147 expression was widely expressed in the 3 different compartments (tumor, stroma, and overlying epithelium). There was a trend toward high expression (grade 3 and grade 4) being more common in the tumor cells compared stroma and adjacent epithelium, but there was no statistical significance ($P > .05$; Figure 2B). The pattern of CD147 expression was similar between COX-2−positive OSCC (n = 24) and COX-2−negative OSCC (n = 13) (Figure 2C).

In vitro expression of COX-1, COX-2, and CD147 and secretion of PGE_2 in OSCC cell lines

In vitro gene expression can be influenced by exposure to FBS. For this reason, gene expression was evaluated in OSCC cells in serum free conditions (serum deprivation), as well as in cells that were recently reintroduced to serum (serum stimulated). COX-1, COX-2, and CD147 expression was detected at the mRNA level in all OSCC cell lines, but at variable levels. Two-hour serum stimulation upregulated COX-2 in all 3 human cell lines but had no significant effect on COX-1 expression (Figures 3A to 3C).

Focusing on serum-stimulated cells, the 3 cell lines differed in COX-1 expression, with lingual SCC25 cells expressing the most COX-1 mRNA (see Figure 3C). COX-2 and CD147 were consistently expressed across the 3 human cell lines (see Figures 3A and 3B), although there was a trend toward gingival BHY cells having the highest COX-2 and CD147 expression and HN metastasis cells having the least COX-2 and CD147 expression. The results were similar under serum deprivation conditions, except that the difference in CD147 expression between human cell lines was significant (see Figure 3), with BHY cells expressing the most CD147.

HN cells secreted the least amount of PGE_2 (Figure 3D), consistent with the RT-qPCR results, showing that HN cells tended to express the least COX-1 and COX-2 mRNA. SCC25 secreted the most PGE_2 (these cells produced the most COX-1), followed by BHY cells (which expressed the most COX-2). Although there was an interesting trend seen in CD147 expression, COX expression, and PGE2 secretion (HN cells producing the least and BHY tending to have higher COX-2 and CD147 expression), the high levels of PGE_2 secreted by SCC25 did not correlate with the relatively low expression of CD147 in these cells.

DISCUSSION

To our knowledge, this is the first study reporting COX-2 and CD147 expression in the same cohort of OSCC patient samples and cell lines. In the biopsy samples, COX-2 expression was more common in the tumor cells compared with the stromal cells or adjacent epithelial cells. This finding is similar to what was reported by Shibata et al., who found that COX-2 expression was higher in OSCC cells compared with dysplastic lesions and normal gingiva.[37] Studies showing higher COX-2 expression in OSCC tumor tissue compared with dysplastic lesions and adjacent normal tissue have also been reported by Pannone et al.[38] and Cho et al.[39] However, Mauro et al. reported that peak COX-2 expression appears to occur during the dysplastic phase and becomes downregulated in carcinoma, although expression is still increased compared with that in normal gingiva.[40] As expected, in this study, COX-2 was mostly localized to the cytoplasmic compartment, although occasional nuclear staining was also observed. Nuclear localization of COX-2 has been reported in bladder cancer cells, where it was associated with expression of markers of stem cell reprogramming (CD44 v6 and Oct3/4).[41] Additionally, nuclear expression of COX-2 was found to be increased by hypoxia in breast cancer cells in bone metastasis, leading to increased expression of hypoxia inducible factor-1α.[42]

The OSCC biopsy samples were also stained for CD147. The OSCC tissues showed widespread and variable expression of CD147, with no significant differences among the cells of the tumor, stroma, and overlying epithelium. Vigneswaran et al. also reported that CD147 was expressed in normal gingiva as well as in hyperplastic, inflammatory, dysplastic, and malignant lesions, but they did find that expression increased with increasing degrees of dysplasia.[43] Monteiro et al.

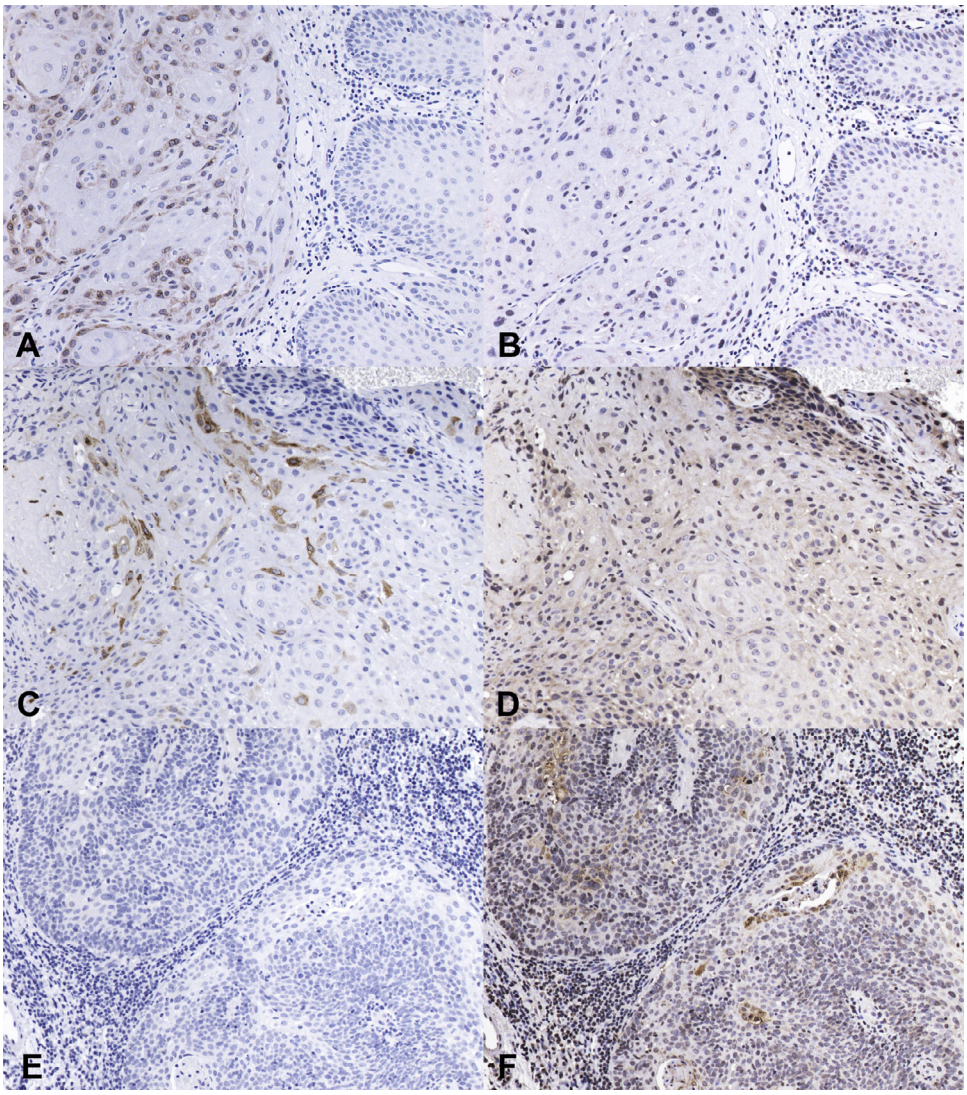

Fig. 1. Cyclooxygenase-2 (COX-2) and cluster of differentiation factor 147 (CD147) in serial sections of human oral squamous cell carcinoma (OSCC). Photomicrographs of immunohistochemistry results using rabbit anti-COX-2 immunoglobulin G (IgG) and goat anti-CD147 IgG in 3 patients with OSCC. The chromogen is diaminobenzinetetrahydrochloride (brown), and the counterstain is hematoxylin (blue). Case 1. **A**, COX-2, **B**, CD147: OSCC cells showed scattered moderate COX-2 expression (grade 2; 10%−50% positive cells) and minimal CD147 expression (negative; less than 1% positive cells). Note the nonmalignant epithelium on the right side of the image, which is negative for COX-2 and CD147 expression. Case 2. **C**, COX-2, **D**, CD147: OSCC cells had variable COX-2 expression (grade 1; 1%−9% positive cells) and widespread moderate CD147 expression (grade 4; mostly moderate with less than 50% heavily-stained cells). Case 3. **E**, COX-2, **F**, CD147: OSCC cells were negative for COX-2 expression, but demonstrated widespread light-to-moderate CD147 signal (grade 3; mostly light with less than 50% moderately-stained cells). In general, COX-2 localization was chiefly cytoplasmic with infrequent nuclear signal. CD147 expression was generally cytoplasmic and membranous with variable nuclear signal. CD147 expression in OSCC appeared to be independent of COX-2 expression.

found CD147 expression in OSCC tumor cells and normal mucosa adjacent to tumors, with the signal localizing to cell membranes as well as the cytoplasm.[30] The present study also showed cytoplasmic and membrane expression of CD147 in OSCC, in addition to instances of nuclear localization. Although the membrane-bound form of CD147 is well known (this form is important for activating MMPs and contributing to tumor invasiveness), it should be noted that intracellular and soluble forms of CD147 also exist.[44] Cytoplasmic and membranous localization of CD147 has been reported in primary lung tumors,[45] and a recent study revealed that the cytoplasmic fragment of CD147 can be cleaved and localized to the nucleus of hepatocellular carcinoma cells, contributing to chemoresistance via autophagy.[46] The significance of subcellular

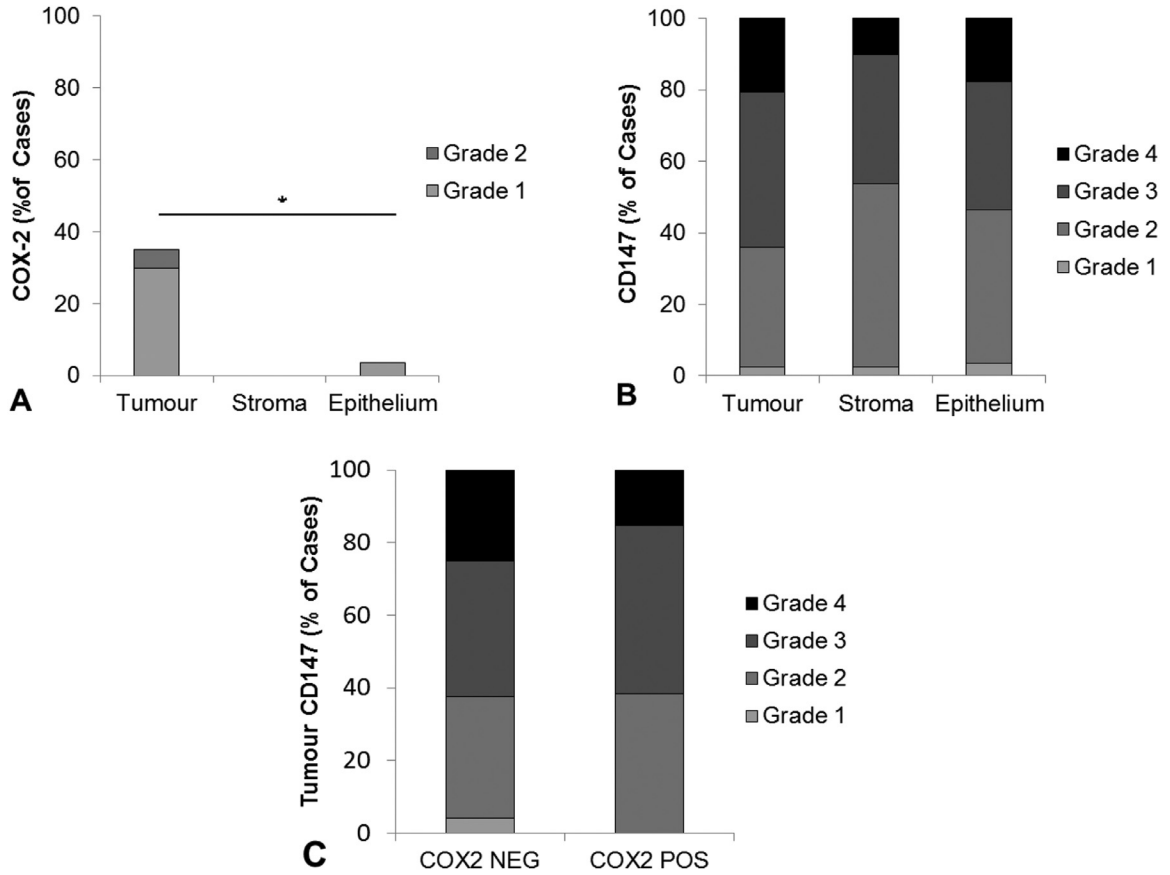

Fig. 2. Expression of cyclooxygenase-2 (COX-2) and cluster of differentiation factor 147 (CD147) in oral squamous cell carcinoma (OSCC), shown with use of immunohistochemical grading system. The OSCC study set was composed of 39 samples, 28 of which included adjacent oral epithelium. **(A)** COX-2 expression by tissue compartment. Each bar represents the percentage of cases that were considered positive for COX-2 expression within each compartment (tumor cells, stroma, and adjacent epithelium). Thirty-seven slides were evaluated (tissue was lost from 2 samples during processing). Each bar is subdivided to demonstrate the percentage of cases assigned to each grade. COX-2 expression was highest in the tumor cells. **(B)** CD147 expression by tissue compartment: Each bar represents the percentage of cases that were considered positive for CD147 expression within each compartment. Thirty-nine slides were evaluated. Each bar is subdivided to demonstrate the percentage of cases assigned to each grade. CD147 expression was variable across all biopsy tissues, with no significant differences between compartments. **(C)** Expression of CD147 in COX-2 positive and COX-2 negative OSCC biopsies. Twenty-four cases had positive COX-2 expression (grades 1 and 2), and 13 cases were COX-2 negative (grade 0). Each bar represents the percentage of positive CD147 cases within the COX-2 positive and COX-2 negative groups. There was no significant difference in CD147 expression. All statistical comparisons were made by using Fisher's exact test (*P value $< .05$).

CD147 localization was not determined in this study but would be an interesting topic to explore in future OSCC research.

Some of the challenges in comparing immunohistochemistry results from different studies arise because of varying study designs. For example, this study compared expression of COX-2 and CD147 expression in OSCC cells with that in adjacent epithelium that bore no morphologic features of malignancy. This provides nontumor tissue that is identical to the tumor tissue in terms of tissue processing, patient signalment, and risk factors. However, these adjacent tissues likely harbor early genetic changes because of exposure to carcinogens, as well as other changes attributed to regional inflammation, which could explain the similar CD147 signal between adjacent nonmalignant tissue and OSCC tissue.

A statistically significant relationship between COX-2 and CD147 expression was not observed with the use of immunohistochemistry. This is in contrast to the findings of a study in hypopharyngeal carcinoma.[33] There were differences in protocols, but the differences in the biology of hypopharyngeal SCC compared with that of OSCC may have also been a contributing factor. Geographic differences in risk factors and genetic predispositions may have also played a role, considering that the hypopharyngeal SCC analysis was performed

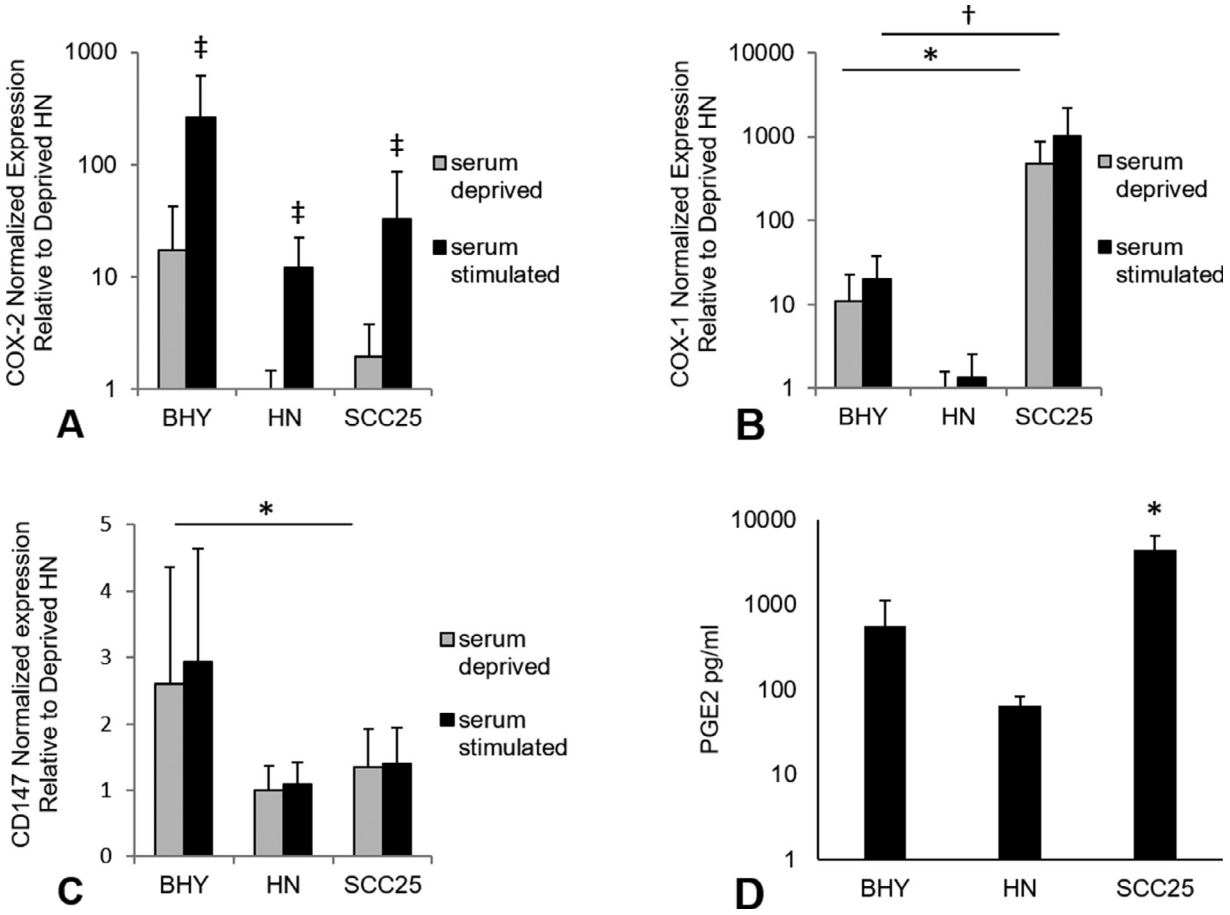

Fig. 3. Expression of cyclooxygenases 1 and 2 (COX-1 and COX-2) and cluster of differentiation factor 147 (CD147) in oral squamous cell carcinoma (OSCC) using reverse transcriptase-quantified polymerase chain reaction (RT-qPCR). **(A)** RT-qPCR for (COX-2) mRNA expression in human OSCC. Each bar represents the mean fold-increase in COX-2 mRNA compared with serum deprived HN cells. Two-hour serum exposure significantly stimulated COX-2 expression in all 3 cell lines. Although there was a trend toward increased COX-2 expression in BHY cells, it was not statistically significant. **(B)** RT-qPCR for COX-1 mRNA expression in human OSCC. Each bar represents the mean fold-increase in COX-1 mRNA compared with serum deprived HN cells. There was no significant effect of serum exposure on COX-1 expression. Expression of COX-1 differed among the 3 cell lines in serum deprived (*) and stimulated (†) conditions, with SCC25 cells expressing the most COX-1. **(C)** RT-qPCR for CD147 mRNA expression in human OSCC. Each bar represents the mean fold-increase in CD147 mRNA compared with serum deprived HN cells. There was no significant effect of serum exposure on CD147 expression. Expression of CD147 differed among the 3 cell lines only in serum deprived (*) conditions, with BHY cells expressing the most. BHY also expressed the most CD147 under serum stimulation, but the results were not statistically significant. **(D)** Enzyme-linked immunosorbent assay detection of prostaglandin E_2 (PGE_2) in human OSCC cell lines. Each bar represents mean PGE_2 concentration in the conditioned medium (pg/mL per 100,000 cells). HN cells secreted the least amount of PGE_2 and SCC25 secreted the most PGE2. All statistical comparisons of RT-qPCR data were made by using Kruskal-Wallis test. (*serum deprived, P value $< .05$; †serum-stimulated, P value $< .05$; ‡serum-deprived compared with serum-stimulated, P value $< .05$). PGE_2 concentrations were log-transformed prior to analysis using 1-way analysis of variance and Bonferroni post hoc test (*P value $<.05$).

in Chinese patient samples in the study by Yang et al. and in Canadian patient samples in the present study.

The immunohistochemistry study of patient samples was accompanied by gene expression analysis in 3 human OSCC cell lines representing different presentations of the disease: bone-invasive gingival OSCC (BHY), lingual OSCC (SCC25), and a lymph node metastasis that arose from the soft palate (HN). All 3 cell lines expressed detectable COX and CD147 mRNA and secreted PGE_2, which is consistent with the findings of previous studies.[13,47-49] Results from this study suggest a possible inverse relationship between COX-1 and COX-2 expression, with gingival BHY cells having relatively high COX-2 expression and relatively low COX-1 expression, and the opposite being true for the lingual SCC25 cells. This is consistent with the work of Pannone et al., who reported a similar inverse relationship between COX-1 and COX-2 in 22 patient samples.[50]

Simultaneous evaluation of the 3 OSCC cell lines revealed interesting patterns of expression regarding COX-1, COX-2, and CD147. SCC25 cells are from a lingual OSCC that were previously shown to express relatively high COX-1.[51] In this study, SCC25 cells expressed the most COX-1 compared with BHY and HN cells, with HN expressing the least. The fact that HN cells also expressed the least CD147 might have suggested a relationship between COX-1 and CD147 expression, but it was the BHY cells that expressed the most CD147 (instead of the high COX-1 expressing SCC25 cells). The higher expression of CD147 in BHY cells compared with HN cells is corroborated by a previous study reporting a similar CD147 expression pattern in BHY and HN cells on flow cytometry.[13]

There was an interesting trend in COX-2 expression being similar to CD147 expression, although the relationship lacked statistical significance. Specifically, BHY tended to have more COX-2 and CD147 expression, and HN tended to have the least. A causal relationship between COX-2 and CD147 expression has been suggested in other studies, such as the observation that COX-2 expression in macrophages can modulate the production of CD147 in a PGE_2-dependent manner.[29] Another study involving macrophages revealed that angiotensin II can upregulate CD147 expression via the COX-2−PGE2 signal transduction pathway.[52]

BHY cells had been previously shown to express COX-2 and be responsive to COX-2 inhibition,[53] and they demonstrated the ability to induce osteoclastic bone resorption in a mouse model.[54,55] Although the invasive nature of BHY cells has been attributed to their expression of parathyroid hormone-related protein,[56] it may be that expression of CD147 and COX-2 in BHY cells also contributes to its bone invasive phenotype. Our study on a spontaneous animal model of invasive OSCC revealed similar findings. For example, bone invasive SCCF2 cells, derived from a gingival OSCC from a domestic cat, expressed CD147 and robust COX-2 expression.[57] Despite arising from different species, these 2 bone-invasive gingival OSCC cell lines express parathyroid hormone-related protein, an inducer of local bone loss, whose expression has been shown to be enhanced by PGE_2.[54,58-60]

HN cells were derived from lymph node metastases and have been shown to be capable of spreading to lungs, kidneys, and cervical lymph nodes in a mouse model.[13] In this study, HN had the lowest CD147, COX-2, and COX-1 expression. Although invasive and metastatic behavior have been correlated with COX-2 and CD147, it may not be surprising that the metastatic HN cells had relatively low COX-2 and CD147 because Mauro et al. reported that COX-2 levels drop as OSCC advances from dysplasia to carcinoma,[40] and Erdem et al. speculated that CD147 may be more important for local invasion rather than distant metastasis.[13]

It was anticipated that the cells expressing the most COX-2 would also secrete the most PGE_2. In contrast, BHY cells[57] did not secrete the most PGE_2 despite strong COX-2 expression. In this study, the cell line that secreted the most PGE_2 was the cell line that expressed the most COX-1—the lingual OSCC cell line SCC25. It should be pointed out that a similar pattern was observed in a natural feline model, with lingual feline OSCC cells (SCCF3) also demonstrating the highest COX-1 expression and PGE2 secretion.[57] Of the 2 COX enzymes, the literature puts an emphasis on the role of COX-2 in OSCC and many other types of cancer, but it appears that COX-1 should still be considered a significant source of tumor-derived PGE_2. This finding is consistent with the findings of Bottone et al., who reported that COX-1 inhibitors were more effective than COX-2 inhibitors against colon cancer.[61] Additionally, the study by Pannone et al., who investigated COX-1 and COX-2 expression in human OSCC, also concluded that COX-1 should be considered a therapeutic target in the management of OSCC.[50]

There have been other examples of discrepancy between COX-2 and PGE_2 levels. For example, human colonic carcinoma-116 and human nasal squamous cell carcinoma-2650 cell lines had low or absent PGE_2 secretion despite high COX-2 expression, as demonstrated through immunohistochemistry and Western blotting.[62] It is important to remember that COX-1 expression and COX-2 expression are not the only factors determining PGE_2 synthesis and secretion. Cervantes-Madrid et al. speculated that the FosB transcription factor regulates COX-2 expression in colorectal cancer cells without affecting PGE_2 or COX-1 expression.[63] Despite increased COX-2 expression, PGE_2 secretion may be hampered by reduced expression of PGE_2 synthase (which is downstream of COX enzymes and converts prostaglandin H2 to PGE_2) or increased activity of 15-hydroxyprostaglandin dehydrogenase, an enzyme which inactivates PGE_2,[64] so it will be important to investigate these enzymes in future studies.

CONCLUSIONS

This study confirms the expression of COX-1, COX-2, and CD147, along with PGE2 secretion, in OSCC cells in vitro, at varying levels and in a cell line-dependent manner. This variation is not surprising, given the range of COX-2 and CD147 expression demonstrated in immunohistochemistry studies of patient samples. The data suggest that the AA pathway and CD147 expression may be independently regulated, representing 2 pathways that might serve as promising targets, rather than 2 participants in a single mechanism.

Furthermore, COX-1 may be a significant source of tumor-derived PGE_2 in OSCC cells, justifying further investigation of COX-1 as a possible therapeutic target for OSCC to avoid the undesirable side effects of COX-2 specific inhibitors. Future studies should evaluate other important contributors to these pathways, including prostaglandin receptors, PGE_2 synthases, and MMPs. Given the complexity of OSCC tumors, future studies should include cocultures incorporating elements of the tumor microenvironment, with increasing use of naturally occurring in vivo models.

ACKNOWLEDGMENTS

The authors are thankful to Spencer Greenwood (Department of Biomedical Sciences, Atlantic Veterinary College) for assistance with RT-qPCR. This study would not be possible without the support of Health PEI Laboratory Services and the technical assistance of Krista Eveleigh.

REFERENCES

1. Warnakulasuriya S. Global epidemiology of oral and oropharyngeal cancer. *Oral Oncol*. 2009;45:309-316.
2. Carreras-Torras C, Gay-Escoda C. Techniques for early diagnosis of oral squamous cell carcinoma: systematic review. *Med Oral Patol Oral Cir Bucal*. 2015;20:e305-e315.
3. Canadian Cancer Society's Advisory Committee on Cancer Statistics. *Canadian Cancer Statistics 2016*. Toronto, Ontario: Canadian Cancer Society; 2016.
4. Johnson N. Tobacco use and oral cancer: a global perspective. *J Dent Educ*. 2001;65:328-339.
5. Canadian Cancer Society's Advisory Committee on Cancer Statistics. *Canadian Cancer Statistics 2017*. Toronto, Ontario: Canadian Cancer Society; 2017.
6. Torre LA, Bray F, Siegel RL, Ferlay J, Lortet-Tieulent J, Jemal A. Global cancer statistics, 2012. *CA Cancer J Clin*. 2015;65:87-108.
7. de Camargo Cancela M, Voti L, Guerra-Yi M, Chapuis F, Mazuir M, Curado MP. Oral cavity cancer in developed and in developing countries: population-based incidence. *Head Neck*. 2010;32:357-367.
8. Siegel R, Naishadham D, Jemal A. Cancer statistics, 2013. *CA Cancer J Clin*. 2013;63:11-30.
9. Myers LL, Sumer BD, Truelson JM, et al. Impact of treatment sequence of multimodal therapy for advanced oral cavity cancer with mandible invasion. *Otolaryngol Head Neck Surg*. 2011;145:961-966.
10. Fukuhara T, Fujiwara K, Fujii T, et al. Usefulness of chest CT scan for head and neck cancer. *Auris Nasus Larynx*. 2015;42:49-52.
11. Morita Y, Hata K, Nakanishi M, Nishisho T, Yura Y, Yoneda T. Cyclooxygenase-2 promotes tumor lymphangiogenesis and lymph node metastasis in oral squamous cell carcinoma. *Int J Oncol*. 2012;41:885-892.
12. Morita Y, Morita N, Hata K, et al. Cyclooxygenase-2 expression is associated with vascular endothelial growth factor-c and lymph node metastasis in human oral tongue cancer. *Oral Surg Oral Med Oral Pathol Oral Radiol*. 2014;117:502-510.
13. Erdem NF, Carlson ER, Gerard DA, Ichiki AT. Characterization of 3 oral squamous cell carcinoma cell lines with different invasion and/or metastatic potentials. *J Oral Maxillofac Surg*. 2007;65:1725-1733.
14. Kalinski P. Regulation of immune responses by prostaglandin E2. *J Immunol*. 2012;188:21-28.
15. Smith WL. The eicosanoids and their biochemical mechanisms of action. *Biochem J*. 1989;259:315-324.
16. Funk CD. Prostaglandins and leukotrienes: advances in eicosanoid biology. *Science*. 2001;294:1871-1875.
17. Nasry WHS, Rodriguez-Lecompte JC, Martin CK. Role of COX-2/PGE2 mediated inflammation in oral squamous cell carcinoma. *Cancers (Basel)*. 2018;10. pii:E348.
18. Li S, Lee YA, Li Q, et al. Oral lesions, chronic diseases and the risk of head and neck cancer. *Oral Oncol*. 2015;51:1082-1087.
19. Jia-Jun T, Su-Mei L, Liang Y, et al. Nimesulide inhibited the growth of hypopharyngeal carcinoma cells via suppressing Survivin expression. *Head Neck Oncol*. 2012;4:7.
20. Nikitakis NG, Hamburger AW, Sauk JJ. The nonsteroidal anti-inflammatory drug sulindac causes down-regulation of signal transducer and activator of transcription 3 in human oral squamous cell carcinoma cells. *Cancer Res*. 2002;62:1004-1007.
21. Hanif R, Pittas A, Feng Y, et al. Effects of nonsteroidal anti-inflammatory drugs on proliferation and on induction of apoptosis in colon cancer cells by a prostaglandin-independent pathway. *Biochem Pharmacol*. 1996;52:237-245.
22. Kao J, Genden EM, Chen CT, et al. Phase 1 trial of concurrent erlotinib, celecoxib, and reirradiation for recurrent head and neck cancer. *Cancer*. 2011;117:3173-3181.
23. Zhao XL, Sun T, Che N, et al. Promotion of hepatocellular carcinoma metastasis through matrix metalloproteinase activation by epithelial-mesenchymal transition regulator Twist1. *J Cell Mol Med*. 2011;15:691-700.
24. Deryugina EI, Quigley JP. Matrix metalloproteinases and tumor metastasis. *Cancer Metastasis Rev*. 2006;25:9-34.
25. Yu Q, Stamenkovic I. Cell surface-localized matrix metalloproteinase-9 proteolytically activates TGF-beta and promotes tumor invasion and angiogenesis. *Genes Dev*. 2000;14:163-176.
26. Biswas C, Zhang Y, DeCastro R, et al. The human tumor cell-derived collagenase stimulatory factor (renamed EMMPRIN) is a member of the immunoglobulin superfamily. *Cancer Res*. 1995;55:434-439.
27. Koch C, Staffler G, Huttinger R, et al. T cell activation-associated epitopes of CD147 in regulation of the T cell response, and their definition by antibody affinity and antigen density. *Int Immunol*. 1999;11:777-786.
28. Zhu P, Lu N, Shi ZG, et al. CD147 overexpression on synoviocytes in rheumatoid arthritis enhances matrix metalloproteinase production and invasiveness of synoviocytes. *Arthritis Res Ther*. 2006;8:R44.
29. Cipollone F, Prontera C, Pini B, et al. Overexpression of functionally coupled cyclooxygenase-2 and prostaglandin E synthase in symptomatic atherosclerotic plaques as a basis of prostaglandin E(2)-dependent plaque instability. *Circulation*. 2001;104:921-927.
30. Monteiro LS, Delgado ML, Ricardo S, et al. EMMPRIN expression in oral squamous cell carcinomas: correlation with tumor proliferation and patient survival. *Biomed Res Int*. 2014;2014:905680.
31. Papadimitropoulou A, Mamalaki A. The glycosylated IgII extracellular domain of EMMPRIN is implicated in the induction of MMP-2. *Mol Cell Biochem*. 2013;379:107-113.
32. Dean NR, Newman JR, Helman EE, et al. Anti-EMMPRIN monoclonal antibody as a novel agent for therapy of head and neck cancer. *Clin Cancer Res*. 2009;15:4058-4065.
33. Yang Q, Liu Y, Huang Y, et al. Expression of COX-2, CD44 v6 and CD147 and relationship with invasion and lymph node metastasis in hypopharyngeal squamous cell carcinoma. *PLoS One*. 2013;8. e71048-e71048.

34. Kirschenbaum A, Klausner AP, Lee R, et al. Expression of cyclooxygenase-1 and cyclooxygenase-2 in the human prostate. *Urology*. 2000;56:671-676.
35. Riethdorf S, Reimers N, Assmann V, et al. High incidence of EMMPRIN expression in human tumors. *Int J Cancer*. 2006;119:1800-1810.
36. Satoh H, Amagase K, Ebara S, Akiba Y, Takeuchi K. Cyclooxygenase (COX)-1 and COX-2 both play an important role in the protection of the duodenal mucosa in cats. *J Pharmacol Exp Ther*. 2013;344:189-195.
37. Shibata M, Kodani I, Osaki M, et al. Cyclo-oxygenase-1 and -2 expression in human oral mucosa, dysplasias and squamous cell carcinomas and their pathological significance. *Oral Oncol*. 2005;41:304-312.
38. Pannone G, Bufo P, Caiaffa MF, et al. Cyclooxygenase-2 expression in oral squamous cell carcinoma. *Int J Immunopathol Pharmacol*. 2004;17:273-282.
39. Cho NP, Han HS, Leem DH, et al. Sulforaphane enhances caspase-dependent apoptosis through inhibition of cyclooxygenase-2 expression in human oral squamous carcinoma cells and nude mouse xenograft model. *Oral Oncol*. 2009;45:654-660.
40. Mauro A, Lipari L, Leone A, et al. Expression of cyclooxygenase-1 and cyclooxygenase-2 in normal and pathological human oral mucosa. *Folia Histochem Cytobiol*. 2010;48:555-563.
41. Thanan R, Murata M, Ma N, et al. Nuclear localization of COX-2 in relation to the expression of stemness markers in urinary bladder cancer. *Mediators Inflamm*. 2012;2012:165879.
42. Maroni P, Matteucci E, Luzzati A, Perrucchini G, Bendinelli P, Desiderio MA. Nuclear co-localization and functional interaction of COX-2 and HIF-1 alpha characterize bone metastasis of human breast carcinoma. *Breast Cancer Res Treat*. 2011;129:433-450.
43. Vigneswaran N, Beckers S, Waigel S, et al. Increased EMMPRIN (CD 147) expression during oral carcinogenesis. *Exp Mol Pathol*. 2006;80:147-159.
44. Grass GD, Toole BP. How, with whom and when: an overview of CD147-mediated regulatory networks influencing matrix metalloproteinase activity. *Biosci Rep*. 2015;36:e00283.
45. Sienel W, Polzer B, Elshawi K, et al. Cellular localization of EMMPRIN predicts prognosis of patients with operable lung adenocarcinoma independent from MMP-2 and MMP-9. *Mod Pathol*. 2008;21:1130-1138.
46. Wu B, Cui J, Yang XM, et al. Cytoplasmic fragment of CD147 generated by regulated intramembrane proteolysis contributes to HCC by promoting autophagy. *Cell Death Dis*. 2017;8:e2925.
47. Moazeni-Roodi A, Allameh A, Harirchi I, Motiee-Langroudi M, Garajei A. Studies on the contribution of Cox-2 expression in the progression of oral squamous cell carcinoma and H-Ras activation. *Pathol Oncol Res*. 2017;23:355-360.
48. Li TJ, Cui J. COX-2, MMP-7 expression in oral lichen planus and oral squamous cell carcinoma. *Asian Pac J Trop Med*. 2013;6:640-643.
49. Qian M, Qian D, Jing H, Li Y, Ma C, Zhou Y. Combined cetuximab and celecoxib treatment exhibits a synergistic anticancer effect on human oral squamous cell carcinoma *in vitro* and *in vivo*. *Oncol Rep*. 2014;32:1681-1688.
50. Pannone G, Sanguedolce F, De Maria S, et al. Cyclooxygenase isozymes in oral squamous cell carcinoma : a real-time RT-PCR study with clinic pathological correlations. *Int J Immunopathol Pharmacol*. 2007;20:317-324.
51. Martin CK, Dirksen WP, Carlton MM, et al. Combined zoledronic acid and meloxicam reduced bone loss and tumour growth in an orthotopic mouse model of bone-invasive oral squamous cell carcinoma. *Vet Comp Oncol*. 2015;13:203-217.
52. Yang L, Ye J, Guo R, et al. The effect of the expression of angiotensin II on extracellular matrix metalloproteinase inducer (EMMPRIN) in macrophages is mediated via the AT1/COX-2/PGE.sub.2 pathway. *Inflammation Res*. 2010;59:1033-1040.
53. Salimi M, Esfahani M, Habibzadeh N, et al. Change in nicotine-induced VEGF, PGE2 AND COX-2 expression following COX inhibition in human oral squamous cancer. *J Environ Pathol Toxicol Oncol*. 2012;31:349-356.
54. Ishikuro M, Sakamoto K, Kayamori K, et al. Significance of the fibrous stroma in bone invasion by human gingival squamous cell carcinomas. *Bone*. 2008;43:621-627.
55. Yamada T, Tsuda M, Ohba Y, Kawaguchi H, Totsuka Y, Shindoh M. PTHrP promotes malignancy of human oral cancer cell downstream of the EGFR signaling. *Biochem Biophys Res Commun*. 2008;368:575-581.
56. Deyama Y, Tei K, Yoshimura Y, et al. Oral squamous cell carcinomas stimulate osteoclast differentiation. *Oncol Rep*. 2008;20:663-668.
57. Nasry WHS, Wang H, Jones K, et al. CD147 and cyclooxygenase expression in feline oral squamous cell carcinoma. *Vet Sci*. 2018;5. pii:E72.
58. Martin CK, Dirksen WP, Shu ST, et al. Characterization of bone resorption in novel in vitro and in vivo models of oral squamous cell carcinoma. *Oral Oncol*. 2012;48:491-499.
59. Yoshida T, Sakamoto H, Horiuchi T, et al. Involvement of prostaglandin E(2) in interleukin-1 alpha-induced parathyroid hormone-related peptide production in synovial fibroblasts of patients with rheumatoid arthritis. *J Clin Endocrinol Metab*. 2001;86:3272-3278.
60. Saito H, Inagaki Y, Tsunenari T, et al. Involvement of cyclooxygenase-2 in the tumor site-dependent production of parathyroid hormone-related protein in colon 26 carcinoma. *Cancer Sci*. 2007;98:1563-1569.
61. Bottone FG Jr, Martinez JM, Alston-Mills B, Eling TE. Gene modulation by Cox-1 and Cox-2 specific inhibitors in human colorectal carcinoma cancer cells. *Carcinogenesis*. 2004;25:349-357.
62. Heller DA, Fan TM, de Lorimier LP, et al. In vitro cyclooxygenase-2 protein expression and enzymatic activity in neoplastic cells. *J Vet Intern Med*. 2007;21:1048-1055.
63. Cervantes-Madrid DL, Nagi S, Asting Gustafsson A. FosB transcription factor regulates COX-2 expression in colorectal cancer cells without affecting PGE2 expression. *Oncol Lett*. 2017;13:1411-1416.
64. Tai HH, Cho H, Tong M, Ding Y. NAD+-linked 15-hydroxyprostaglandin dehydrogenase: structure and biological functions. *Curr Pharm Des*. 2006;12:955-962.

Reprint requests:

Chelsea K. Martin
Department of Pathology and Microbiology
Atlantic Veterinary College
University of Prince Edward Island
Charlottetown, Prince Edward Island
C1A 4P3
Canada
Ckmartin@upei.ca

SUPPLEMENTARY MATERIALS

Results

Primary antibodies and matching isotype control antibodies

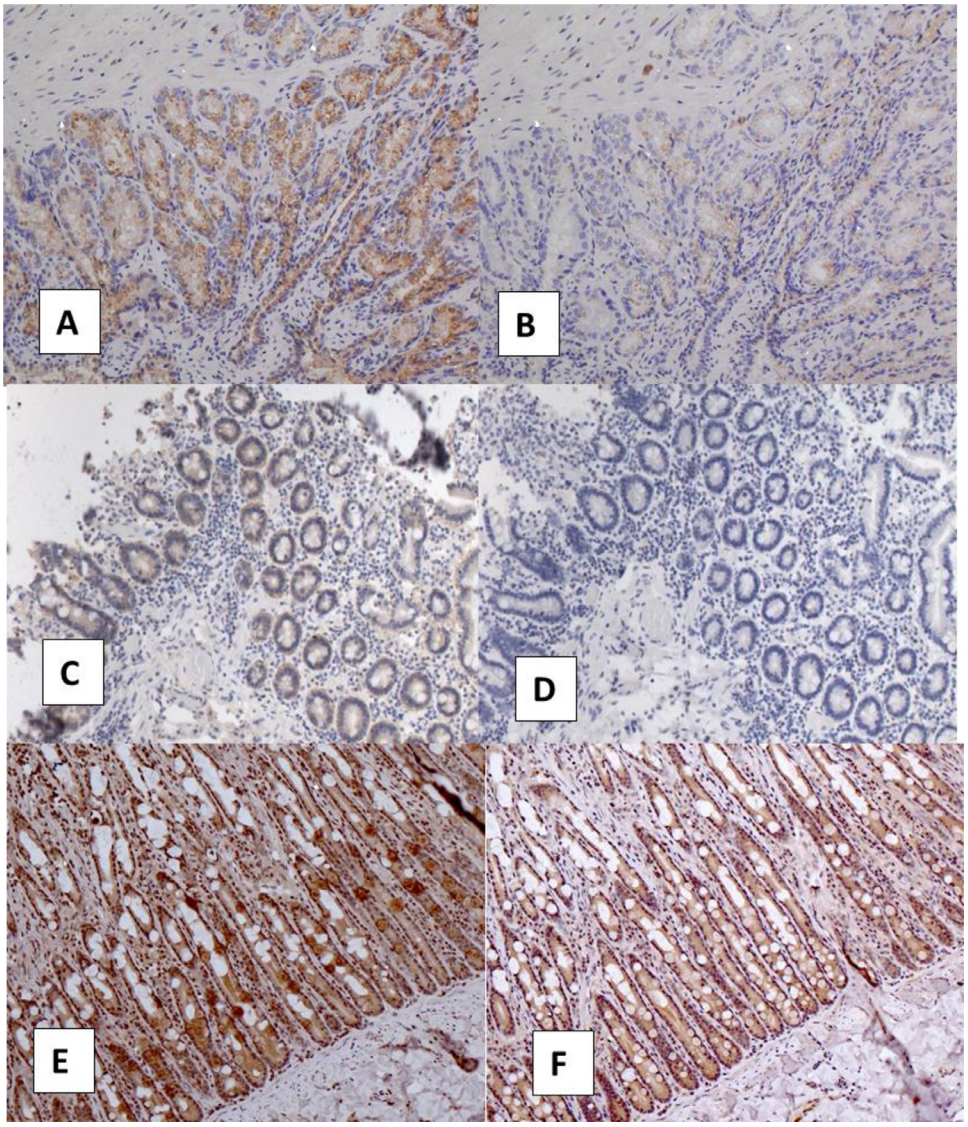

Figure S1. COX-2, CD147 and COX-1 positive and negative controls for immunohistochemistry.

Photomicrographs of IHC staining of COX-2, CD147 and COX-1 positive and negative controls **A.** The rabbit-anti-COX-2 IgG concentration was 1:200, which gave positive signal on human seminal vesicle epithelial cells (positive control tissue) with moderate cytoplasmic COX-2 signal in glandular epithelial cells. **B.** Replacement of the antibody with normal rabbit IgG significantly reduced the signal. Remaining light brown color was interpreted as endogenous pigment (lipofuscin) typical of this tissue. **C.** A 1:100 dilution of goat anti-CD147 gave positive signal in human small intestine enterocytes (positive control tissue) with mild to moderate cytoplasmic CD147 signal in enterocytes. **D.** Replacement of the CD147 antibody with control goat IgG significantly reduced the signal. **E.** Rabbit anti-COX-1 anti-serum diluted to 1:100 achieved positive signal in feline intestinal goblet cells (positive control). **F.** Replacing the COX-1 anti-serum with normal rabbit serum reduced staining in goblet cells but a high amount of nonspecific stain that was indistinguishable from the COX-1 anti-serum in human OSCC COX-1 immunohistochemistry was not selected for further analysis

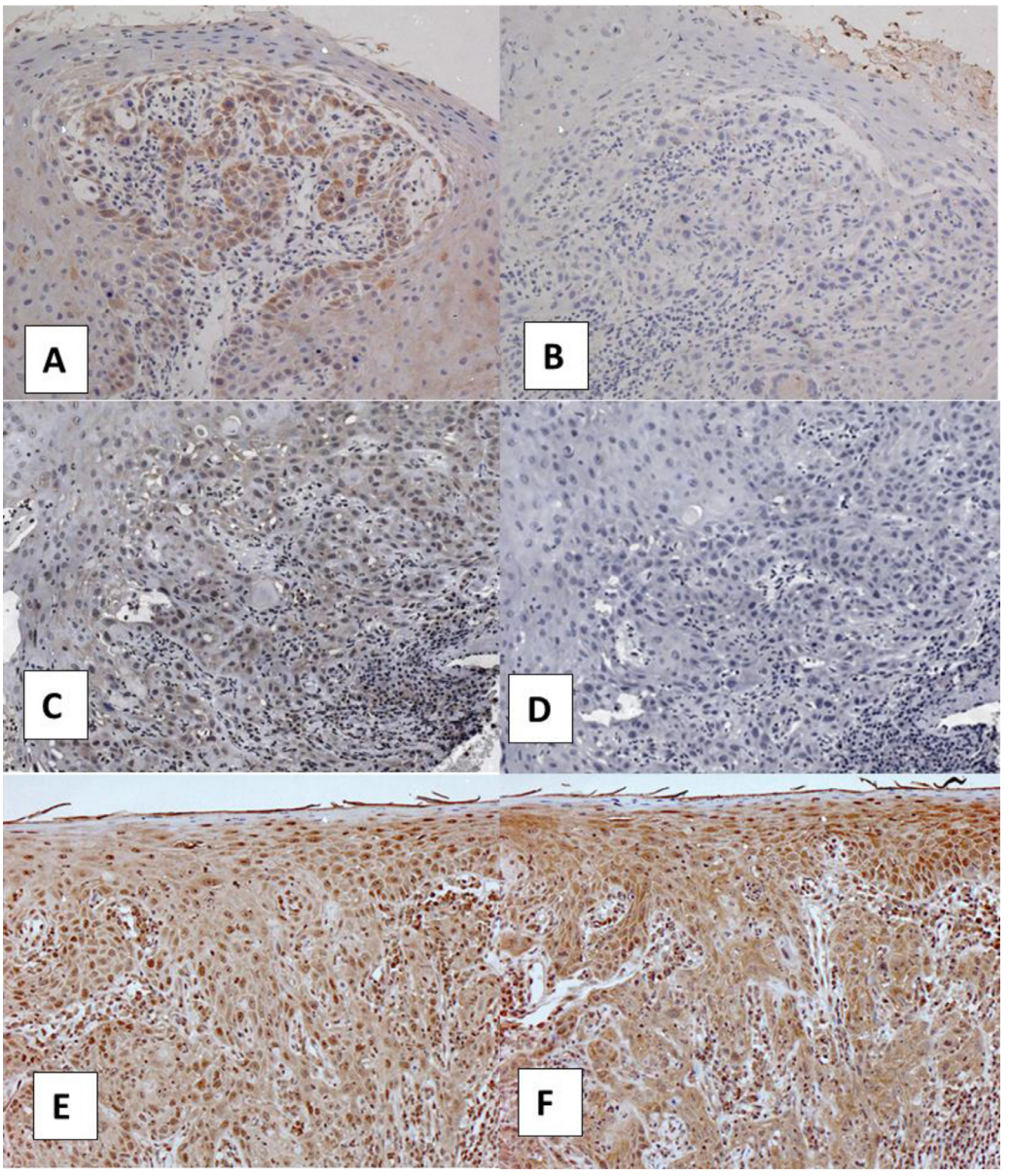

Figure S2. COX-2, CD147 and COX-1 positive and negative controls OSCC for immunohistochemistry.

Photomicrographs of IHC staining of COX-2, CD147 and COX-1 positive and negative controls **A.** COX-2 antibody on a human OSCC biopsy with mild gingival staining and moderate OSCC staining. **B**. Replacement of the antibody with peptide significantly reduced signal. **C.** CD147 antibody on a human OSCC biopsy with moderate staining in OSCC cells and in surrounding stroma**. D.** Replacement of the antibody with normal goat IgG significantly reduced signal. **E.** Human OSCC had widespread heavy staining using COX-1 antiserum. **F.** The same human OSCC biopsy had similar staining with normal rabbit serum, demonstrating that the protocol was not specific for COX-1 expression (background signal was indistinguishable from positive signal).

Table S1. Screened human reference genes

Predesigned Reference Genes H96 Panel (Bio-Rad) Human Gene Name
RPL13A
RPLP0
GUSB
G6PD
TBP
RPS18
HPRT1
GAPDH
B2M
ACTB
TFRC
YWHAZ
HMBS
PGK1

Table S2. Human primers

Primer Assay Name	Unique Assay ID (Bio-Rad)	Amplicon Length	Spans Intron?
*hPTGS1	qHsaCID0009735	100	No
*hPTGS2	qHsaCED0042341	118	No
*hCD147	qHsaCED0056835	62	No
hTBP	qHsaCID0007122	120	Yes
**hRPS18	qHsaCED0037454	67	No
**hHPRT1	qHsaCID0016375	90	Yes
hGAPDH	qHsaCED0038674	117	No
hB2M	qHsaCID0015347	123	Yes

*Genes of interest: PTGS1 (COX-1), PTGS2 (COX-2) and CD147. Other genes listed are candidate reference (housekeeping) genes that were tested.

**Reference genes that were selected for normalization of the data after evaluation of M and CV values.